

# Evidence of cross-correlation between the CMB lensing and the $\gamma$ -ray sky

Nicolao Fornengo,<sup>1,2</sup> Laurence Perotto,<sup>3</sup> Marco Regis,<sup>1,2,\*</sup> and Stefano Camera<sup>4</sup>

<sup>1</sup>*Dipartimento di Fisica Teorica, Università di Torino, I-10125 Torino, Italy*

<sup>2</sup>*Istituto Nazionale di Fisica Nucleare, Sezione di Torino I-10125 Torino, Italy*

<sup>3</sup>*LPSC, Université Grenoble-Alpes, CNRS/IN2P3,*

*53, rue des Martyrs 38026 Grenoble Cedex, France*

<sup>4</sup>*CENTRA, Instituto Superior Técnico, Universidade de Lisboa, Lisboa, Portugal*

(Dated: June 17, 2022)

We report the measurement of the angular power spectrum of cross-correlation between the unresolved component of the *Fermi*-LAT  $\gamma$ -ray sky-maps and the CMB lensing potential map reconstructed by the *Planck* satellite. The matter distribution in the Universe determines the bending of light coming from the last scattering surface. At the same time, the matter density drives the growth history of astrophysical objects, including their capability at generating non-thermal phenomena, which in turn give rise to  $\gamma$ -ray emissions. The *Planck* lensing map provides information on the integrated distribution of matter, while the integrated history of  $\gamma$ -ray emitters is imprinted in the *Fermi*-LAT sky maps. We report here the first evidence of their correlation (at  $3.2\sigma$  C.L.). We find that the multipole dependence of the cross-correlation measurement is in agreement with current models of the  $\gamma$ -ray luminosity function for AGN and star forming galaxies. Moreover, its amplitude can in general be matched only assuming that these extra-galactic emitters are also the bulk contribution of the measured isotropic  $\gamma$ -ray background (IGRB) intensity. This leaves little room for a big contribution from galactic sources to the IGRB measured by *Fermi*-LAT, pointing toward a direct evidence of the extragalactic origin of the IGRB.

PACS numbers: 98.80.-k, 98.80.Es, 98.70.Rz, 98.62.Sb

## I. INTRODUCTION

The weak gravitational lensing by large scale structures imprints the integrated dark matter distribution onto the cosmic microwave background (CMB) anisotropies. It results in a remapping of the CMB observables, which depends on the line-of-sight integral of the gravitational potential, with a broad kernel peaking at a redshift  $z \sim 2$ , and which is referred to as the *lensing potential* [1] (see also Ref. [2] for a review). This process perturbs the statistical properties of the CMB observables, which are primarily very close to Gaussian fields. This non-Gaussian signature can be exploited to extract the lensing potential from the CMB maps [3]. Using such a technique, the *Planck* Collaboration obtained a unique nearly all-sky map of the lensing potential from a combination of temperature maps [4], which provides us with an estimate of the matter distribution, mainly sensitive to halos located at  $1 \lesssim z \lesssim 3$ .

On the other hand, the accretion of baryonic matter in halos also creates active astrophysical structures. They can host violent phenomena, such as, e.g., supernova explosions and relativistic outflows, which are able to accelerate particles to high-energies. Particles with GeV-TeV energy interacting with the ambient medium emit  $\gamma$ -

ray radiation, mostly by means of production and decay of neutral pions, inverse Compton scattering, and non-thermal bremsstrahlung. In addition, the same dark matter which forms the halos could produce  $\gamma$ -rays, through its self-annihilation or decay. In the past few decades, the all-sky diffuse  $\gamma$ -ray emission has been measured, but its origin and composition remain key open questions in high-energy astrophysics. The featureless energy spectrum of the isotropic  $\gamma$ -ray background (IGRB) [5] and its flat angular power spectrum (APS) [6] make the IGRB identification a complex task.

In this work, we first show that the lensing potential map estimated by *Planck* and the  $\gamma$ -ray sky observed by *Fermi*-LAT do correlate, by reporting a measurement of their cross-correlation APS. This stems from their common origin associated to extragalactic structures, and we discuss the extragalactic  $\gamma$ -ray background (EGB) properties which can explain the measurement.

The adopted cosmological model throughout this paper is the six-parameter  $\Lambda$ CDM *Planck* best fitting model reported in [7].

## II. DATA AND ANALYSIS

We use the  $\gamma$ -ray measurements obtained by the *Fermi*-LAT in its first 68 months of operations, from early August 2008 to late April 2014. We have processed the data

\* Corresponding author (regis@to.infn.it)

with the FERMISCIENCE TOOLS version v9r32p5, using the Pass7-reprocessed instrument response functions for the CLEAN event class (P7REP\_CLEAN\_V15) for both FRONT and BACK conversion types of events, which have been taken together. We have selected photon counts from 700 MeV to 300 GeV, subdivided into 70 energy bins (uniform in log scale) and mapped with a pixel size of  $0.125^\circ$  (suitable for subsequent HEALPIX projection with  $N_{\text{side}} = 512$ ). The *Fermi-LAT* exposure maps have been derived on the same energy grid and resolution, and we adopted a step size  $\cos \theta = 0.025$ , in order to have sufficiently refined exposures. From the count and exposure map cubes, we have finally derived the full-sky flux maps. For the cross-correlation analysis, we have grouped the energy sections in 6 bins (with boundaries at: 0.7, 0.99, 2.0, 5.1, 10.2, 48.7, 300 GeV).

The maps are contaminated by the galactic foreground: since we are interested in the extragalactic signal only, the maps have been cleaned by subtracting the *Fermi-LAT* galactic model `gll_iem_v05`, which can be obtained from Ref. [8].

We use the CMB lensing potential map provided by the *Planck* Collaboration as part of its March 2013 public data release. The methodology that was used to obtain this map, which is referred to as  $\hat{\phi}$ , is described in Ref. [4]. For our analysis, we build a map using the convergence harmonic coefficients  $\kappa_{\ell m} = \ell(\ell + 1)/2 \hat{\phi}_{\ell m}$  to reduce the steepness of the APS as a function of multipoles.

We then mask regions contaminated by galactic foreground and extragalactic sources. We use the *Planck* baseline lensing analysis 70% galactic mask, which accounts for the carbon-monoxide emission lines, the nearby galaxies and the galactic dust thermal emission, apodized over  $5^\circ$  (in order to mitigate the multipole mixing due to the mask). For the  $\gamma$ -ray maps we prepare a mask combining the *Planck* galactic mask, a cut for galactic latitudes  $|b| < 25^\circ$  and excluding a  $1^\circ$  angular radius around each source in the 2-year *Fermi-LAT* catalog (2FGL) [9]. The mask is apodized over  $3^\circ$  and the resulting effective sky fraction available is about 25%. We explored different sets of galactic masks and apodizations, finding consistent results.

The cross-correlation APS between the *Planck* lensing map and the *Fermi-LAT*  $\gamma$ -ray map is estimated using a pseudo- $C_\ell$  approach [10]. To this aim, we make use of the publicly available tool *PolSpice* [11, 12]. Although the method of Refs. [11, 12] properly deconvolves the signal APS from mask effects, it is known not to be a minimum variance algorithm [13]. Thus the associated covariance matrix is likely to be an overestimation of the actual uncertainty, and the significances reported throughout the paper can in turn be considered as conservative.

We band-pass filter the cross-correlation APS in the

multipole range  $40 < \ell < 400$  in order to reduce possible contamination from systematic effects. This multipole range was defined in Ref. [4] as a confidence interval retaining 90% of the lensing information, with multipoles  $\ell < 40$  requiring large *mean-field* bias corrections. Similarly, multipoles above few hundreds are hardly accessible with the *Fermi-LAT* sensitivity and angular resolution, and low multipoles correspond to the scales where the foreground cleaning has the largest impact [6]. Since the expected signal is predicted to scale as  $1/\ell$  (see next Section), the analysis is performed in terms of  $\ell C_\ell^{(\kappa\gamma)}$ . In order to further mitigate mask mode-mixing, we average the APS in six linear bins of width  $\Delta\ell = 60$ .

First, we measure the cross-correlation APS between the CMB lensing and a single  $\gamma$ -ray map derived from the integrated counts at  $E > 1$  GeV, which is shown in Fig. 1 with blue circles. The reported error bars are the diagonal elements of the covariance matrix obtained from *PolSpice*. We found the off-diagonal terms of the binned covariance matrix to be negligible. In essence, we detect a peak at  $\ell \lesssim 150$ , while at smaller angular scales the data are compatible with a null signal. We define a global significance by further binning the APS in a single bin of width  $\Delta\ell = 120$  (namely,  $40 \leq \ell < 160$ ) and taking the ratio of measured APS over error. It amounts to  $2.1\sigma$ .

Then we consider the combination of the cross-correlation estimates from  $\gamma$ -ray maps in the different energy bins introduced above. Since the EGB spectrum roughly scales with  $E^{-2.4}$  (see inset in Fig. 1), low energy bins have larger statistics. On the other hand, the *Fermi-LAT* point spread function significantly improves at high energy [14], and we expect some information gain by splitting the signal in different energy bins. A minimum variance combination of the 6 single  $E$ -bin  $C_b^{(\gamma^i\kappa)}$  measurements in a given multipole bin  $b$  can be defined as:

$$C_b^{(\kappa\gamma)} = \sum_{i=1}^6 w_i(b) C_b^{(\gamma^i\kappa)}, \quad w_i(b) = N_b \sum_{j=1}^6 [\Gamma_b^{-1}]^{ij}, \quad (1)$$

where  $\Gamma_b^{ij} \equiv \text{Cov}[C_b^{(\gamma^i\kappa)}, C_b^{(\gamma^j\kappa)}]$  is the  $6 \times 6$  sub-matrix for the covariance in the bin  $b$ , and  $N_b = \left( \sum_{ij} [\Gamma_b^{-1}]^{ij} \right)^{-1}$ . Note that, after having checked the stability of our results against the inclusion of the correlation among different multipole bins  $\Gamma_{bb'}^{ij}$ , we choose not to include them for simplicity. We normalize  $C_b^{(\gamma^i\kappa)}$  by means of the factor  $E_i^{2.4}/\Delta E_i$  (with  $E_i = \sqrt{E_{\text{max},i} E_{\text{min},i}}$  and  $\Delta E_i = E_{\text{max},i} - E_{\text{min},i}$ ) to make it approximately flat in energy.

The computation of the full covariance matrix including correlation among different  $E$ -bins is not straightforward. Whereas the correlation terms among different

multipole bins within an  $E$ -bin are provided by PolSpice, we estimate the off-diagonal correlation between the  $E_i$  and  $E_j$  bins (with  $i \neq j$ ) using a two-step process. We first derive a semi-analytic Gaussian approximation (averaged in the multipole bin  $b$ ):

$$\tilde{\Gamma}_b^{ij} = \left\langle \frac{C_\ell^{(\gamma^i \kappa)} C_\ell^{(\gamma^j \kappa)} + \hat{C}_\ell^{(\kappa)} \hat{C}_\ell^{(\gamma^i \gamma^j)}}{(2\ell + 1) f_{\text{sky}}} \right\rangle, \quad (2)$$

where  $C_\ell^{(\gamma^i \kappa)}$  is the cross-correlation APS, estimated using a benchmark theoretical prediction discussed in the next Section. (Note that this term is in any case subdominant in Eq. (2)).  $\hat{C}_\ell^{(\kappa)}$  and  $\hat{C}_\ell^{(\gamma^i)}$  are the auto-correlation APS that we estimate from the corresponding maps using PolSpice and  $\hat{C}_\ell^{(\gamma^i \gamma^j)}$  is the cross-correlation APS between two energy bins  $i$  and  $j$ . As a sanity test, we checked that the noise-subtracted estimate  $C_\ell^{(\gamma^i)} = \hat{C}_\ell^{(\gamma^i)} - (C_N^{(\gamma^i)} / W_\ell^2)$  (where  $C_N$  is the power spectrum of the shot noise and  $W_\ell$  is the beam function) agrees well with the autocorrelation APS reported by the *Fermi-LAT* Collaboration [6]. Similarly, our  $\hat{C}_\ell^{(\kappa)}$  is consistent with theoretical expectations, once corrected for the noise APS provided in the Planck public data release [4]. The factor  $f_{\text{sky}}$  corrects for the effective available fraction of the sky, but Eq. (2) might actually underestimate the impact of masks. To have a more conservative error estimate we derive a scaling coefficient  $M_{i,b}$  from  $\Gamma_b^{ii} = M_{i,b}^2 \tilde{\Gamma}_b^{ii}$ , where  $\Gamma_b^{ii}$  is obtained from PolSpice and  $\tilde{\Gamma}_b^{ii}$  from Eq. (2), and then define the off-diagonal terms of the covariance matrix as  $\Gamma_b^{ij} = M_{i,b} M_{j,b} \tilde{\Gamma}_b^{ij}$ . The reliability of this scaling is further supported by the fact we are using the same mask for all the  $\gamma$ -ray maps.

The combined APS  $C_b^{(\kappa\gamma)}$  of Eq. (1) is shown in Fig. 1 with red squares. They are in fair agreement with the measurement from the integrated map, but, as expected, have smaller error bars (given by  $\sqrt{N_b}$ ). As before, we estimate the significance of the cross-correlation signal considering a single multipole bin at  $40 \leq \ell < 160$ . The statistical evidence amounts to  $3.2\sigma$  C.L..

### III. INTERPRETATION

We now move on to discuss the agreement between theoretical models and the measurements reported in Fig. 1.

In the Limber approximation [15], the theoretical two-point cross-correlation APS can be computed as:

$$C_\ell^{(\kappa\gamma)} = \int \frac{d\chi}{\chi^2} W_\kappa(\chi) W_\gamma(\chi) P_{\kappa\gamma}(k = \ell/\chi, \chi). \quad (3)$$

where  $\chi(z)$  denotes the radial comoving distance,  $W_\kappa$  and  $W_\gamma$  are the window functions for lensing and  $\gamma$  rays,

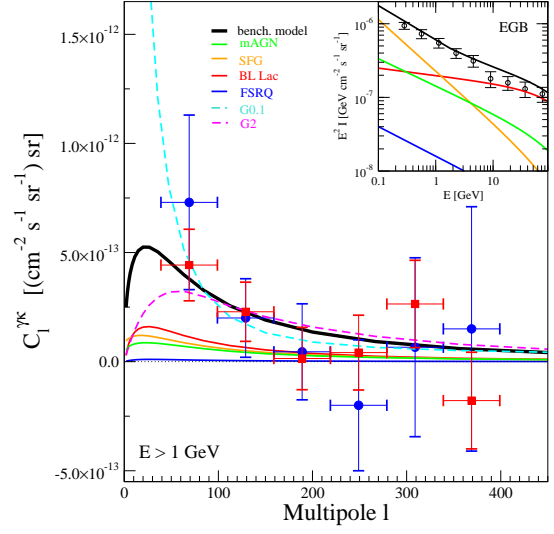


FIG. 1. Cross-correlation APS  $C_\ell^{(\kappa\gamma)}$  as a function of the multipole  $\ell$ , for  $\gamma$ -ray energies  $E > 1$  GeV. The measurements are averaged (linearly in terms of  $\ell C_\ell^{(\kappa\gamma)}$ ) in multipole bins of  $\Delta\ell = 60$ , starting at  $\ell = 40$ . Blue circles refer to the measurements using the  $\gamma$ -ray map integrated for  $E > 1$  GeV, while red squares report the minimum-variance combination of individual energy bin estimates (assuming a spectrum  $\propto E^{-2.4}$ ). The benchmark theoretical model (see text), shown in black, is the sum of the contributions from BL Lac (red), FSRQ (blue), mAGN (magenta), and SFG (orange), multiplied by  $A^{\kappa\gamma} = 1.4$ . We show also two “generic” models G0.1 and G2 with Gaussian  $W(z)$  (normalized to provide the whole EGB above 1 GeV and then multiplied by the factor  $A^{\kappa\gamma}$  described in the text), with peak at  $z_0 = 0.1$  and width  $\sigma_z = 0.1$  (cyan-dashed), and  $z_0 = 2$  and  $\sigma_z = 0.5$  (magenta-dashed), respectively. In the upper inset, we show the EGB benchmark model and *Fermi-LAT* measurement.

and  $P_{\kappa\gamma}$  is the three-dimensional (3D) power-spectrum (PS) of the cross-correlation. For the latter we follow the halo model approach (see, e.g., Ref. [16] for a review), where  $P$  can be split in the one-halo  $P_{1h}$  and two-halo  $P_{2h}$  components as  $P = P_{1h} + P_{2h}$  (see Ref. [17] for their expressions).

The CMB lensing window function is given by [18]:

$$W_\kappa(\chi) = \frac{3}{2} H_0^2 \Omega_m [1 + z(\chi)] \chi \frac{\chi_* - \chi}{\chi_*}, \quad (4)$$

where  $H_0$  is the Hubble constant,  $\Omega_m$  is the matter-density parameter, and  $\chi_*$  is the comoving distance to the last-scattering surface.

The window function for a  $\gamma$ -ray emitter  $i$  is (see, e.g., Ref. [19]):

$$W_{\gamma i}(E, z) = \frac{\int_{\mathcal{L}_{\min}(z)}^{\mathcal{L}_{\max}(z)} d\mathcal{L} \Phi_{\gamma i} \mathcal{L}}{4\pi(1+z)} \exp[-\tau[E(1+z), z]] \quad (5)$$

where  $\mathcal{L}$  is the  $\gamma$ -ray luminosity per unit energy range,  $\Phi_\gamma(\mathcal{L}, z)$  is  $\gamma$ -ray luminosity-function (GLF), and  $\tau$  is the optical depth for absorption [20].

We consider four different extragalactic  $\gamma$ -ray populations: star forming galaxies (SFG), misaligned AGN (mAGN), and two subclasses of blazars, BL Lacertae (BL Lac) and flat spectrum radio quasars (FSRQs). The GLFs of the last three source classes are taken from the best-fit models of, respectively, Refs. [21], [22], and [23]. In the case of SFG we consider the infrared luminosity function from Ref. [24] (adding up spiral, starburst, and SF-AGN populations of their Table 8), and linking  $\gamma$  and infrared luminosities by means of the relation derived in Ref. [25]. The energy spectrum is assumed to be a power-law with spectral indexes  $-2.7$  (SFG),  $-2.37$  (mAGN),  $-2.1$  (BL Lac), and  $-2.4$  (FSRQ).

The model fairly reproduces *Fermi-LAT* measurements for both the EGB (see the upper-right inset of Fig. 1) and the  $\gamma$ -ray autocorrelation APS. For the latter, we found a flat APS (given by the 1-halo term and dominated by BL Lac contribution) with  $C_\ell = 1.5 \times 10^{-17} \text{ cm}^{-4} \text{ s}^{-2} \text{ sr}^{-1}$  for  $E > 1 \text{ GeV}$ .

The cross-correlation power spectrum at the intermediate scales considered here is mostly set by the linear part of the clustering,  $P \simeq P_{2h}$ , which is similar in the various cases (i.e., it is related to the linear total matter PS  $P_{\text{lin}}$ ) except for the specific bias term, with negligible contribution from  $P_{1h}$ . In other words, we approximately have  $C_\ell^{(\kappa\gamma)} = \int d\chi \chi^{-2} W_\kappa(\chi) W_\gamma(\chi) b_{\text{eff}}^{\gamma_i}(z) P_{\text{lin}}(\ell/\chi, \chi)$ , where the “effective” bias of a  $\gamma$ -ray population is:  $b_{\text{eff}}^{\gamma_i}(z) = \int d\mathcal{L} b^{\gamma_i}(\mathcal{L}, z) \Phi_{\gamma_i} \mathcal{L} / (\int d\mathcal{L} \Phi_{\gamma_i} \mathcal{L})$  with  $b^{\gamma_i}(\mathcal{L}, z)$  being the bias between the  $\gamma$ -ray source  $i$  and matter, as a function of luminosity and redshift. To estimate the latter, we use the halo bias  $b_h$  [26] (setting  $b^{\gamma_i}(\mathcal{L}, z) = b_h(M^{\gamma_i}(\mathcal{L}, z))$  and the relation  $M^{\gamma_i}(\mathcal{L}, z)$  (setting the mass of the halo hosting astrophysical objects  $i$  with a certain luminosity  $\mathcal{L}$ ), as described in [27]. The cross-correlation APS predicted in the models of the four  $\gamma$ -ray emitters described above and their collective contribution are shown in Fig. 1.

With the theoretical model at hand we can fit its overall amplitude  $A^{\kappa\gamma}$  by minimizing the  $\chi^2$ , which is computed by means of the full covariance matrix introduced above. The statistical significance of the model is derived computing the  $\Delta\chi^2$  between null signal and best-fit model. We obtain  $A^{\kappa\gamma} = 1.42 \pm 0.47$  with  $3.0\sigma$  significance.

The window functions of the considered  $\gamma$ -ray populations are all peaked at  $z \sim 0.5 - 1$ . To explore in a more general way the kind of  $\gamma$ -ray model preferred by the data, we compute in Fig. 1 the signals from two Gaussian window functions  $W(z) \propto \exp[-(z - z_0)/\sigma_z^2]$ , one peaked at low redshift (model G0.1 with  $z_0 = \sigma_z = 0.1$ ),

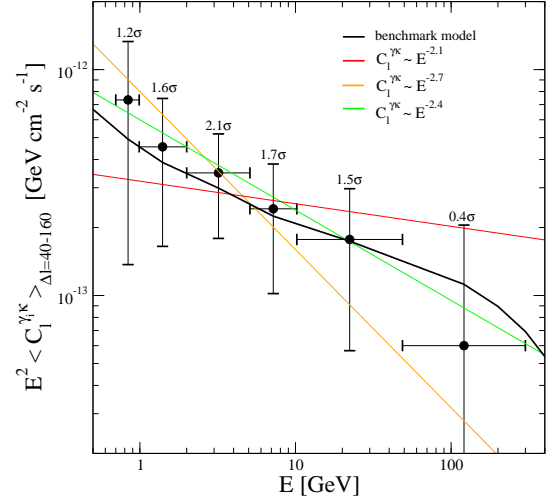


FIG. 2. Energy dependence of the cross-correlation APS. The reported points are for  $E^2 \langle C_\ell^{\gamma\kappa} \rangle_{\Delta\ell=40-120}$ , which is the energy-differential APS of each energy bin  $i$  averaged in the multipole bin  $40 < \ell < 160$  and multiplied by  $E^2$ . Errors are from the diagonal of the covariance matrix and we report the statistical significance of each point. The benchmark theoretical model is shown in black and is multiplied by the energy averaged amplitude  $A^{\kappa\gamma} = 1.4$ .

and one peaked at high redshift (model G2 with  $z_0 = 2$  and  $\sigma_z = 0.5$ ), both normalized to match the *Fermi-LAT* EGB measurement above 1 GeV (and bias modelled as for mAGNs). We found  $A_{G0.1}^{\kappa\gamma} = 2.96 \pm 0.95$  ( $3.1\sigma$ ) and  $A_{G2}^{\kappa\gamma} = 0.91 \pm 0.32$  ( $2.8\sigma$ ). For  $W(z)$  peaked at  $z \gg 1$  the relative contribution of small (more distant) objects with respect to larger objects increases, while no power is detected at small scales (above  $\ell \sim 150$ ). This slightly reduces the statistical significance (although with the current data accuracy we cannot exclude this possibility). On the contrary,  $W(z)$  peaked at low  $z$  would provide the right bump at low  $\ell$ , increasing the statistical significance. However, the large value of the overall amplitude translates into  $\langle b_{\text{eff}} \rangle \sim 3$ , which is typically way too large for a low- $z$  population. This seems to suggest that, in order to reproduce the observed cross-correlation, the bulk of  $\gamma$ -ray contribution to the EGB have to reside at intermediate redshift.

Fig. 2 shows the measured cross-correlation APS for different energy bins and averaged in the multipole bin  $40 < \ell < 160$ . The spectrum is consistent with the benchmark model and similar to the *Fermi-LAT* EGB spectrum, namely the spectral index is close to  $-2.4$ .

#### IV. DISCUSSION AND CONCLUSIONS

We reported the first indication of a cross-correlation between the unresolved  $\gamma$ -ray sky and CMB lensing. The analysis also points towards a direct evidence that the IGRB is of extragalactic origin.

The analysis has been based on the  $\gamma$ -ray data of the first 68 month of operation of the *Fermi-LAT* and on the 2013 public release by the *Planck* Collaboration of the CMB lensing potential map. Current models of AGN and SFG can fit well the amplitude, angular dependence and energy spectrum of the observed APS.

The size of the signal appears to be robust against variations of the analysis assumptions and has a statistical significance of  $3.2\sigma$ . The forthcoming new data releases from the *Planck* Collaboration, expected in the next months, and the *Fermi-LAT* Pass-8 reprocessed events, foreseen for the next year, will allow for a more refined assessment of the signal.

Contaminations from foreground, either real (e.g., a dust or point sources bi-spectrum) or spurious, cannot, at present, be totally excluded. However, we performed the same analysis discussed above with  $\gamma$ -ray maps where the foreground was not subtracted, finding the same central values for the cross-correlation APS, with larger errors (and so lower statistical significance), consistent with the fact that the galactic foregrounds contribute to the error budget but not to the signal. The other argument in favour of the extragalactic interpretation is

that the model of  $\gamma$ -ray populations (built to explain the EGB, and not tuned to the measurement presented here) matches well the data both in features and normalization.

More generically, a population of extragalactic  $\gamma$ -ray emitters following matter clustering at large scales with GLF peaked at intermediate  $z$  and with  $\langle b_{\text{eff}} \rangle \sim 2 - 3$  agrees well with the data, once the associated EGB is normalized to fit the *Fermi-LAT* measurement of the IGRB. On the contrary, if, for example, the contribution to the IGRB is reduced to 50%, the required bias would become  $\langle b_{\text{eff}} \rangle \sim 4 - 6$ , which is likely unrealistically large. This implies that the presented results can be considered as a first direct proof that the majority of the IGRB is emitted by extragalactic structures.

#### ACKNOWLEDGMENTS

We thank D. Maurin for a question which was the actual kick-off of the project, and A. Cuoco for insightful discussions. This work is supported by the research grant *Theoretical Astroparticle Physics* number 2012CPPYP7 under the program PRIN 2012 funded by the Ministero dell'Istruzione, Università e della Ricerca (MIUR), by the research grants *TAsP (Theoretical Astroparticle Physics)* and *Fermi* funded by the Istituto Nazionale di Fisica Nucleare (INFN), and by the *Strategic Research Grant: Origin and Detection of Galactic and Extragalactic Cosmic Rays* funded by Torino University and Compagnia di San Paolo.

- 
- [1] A. Blanchard and J. Schneider, *A&A* **184** (1987) 1.
  - [2] A. Lewis and A. Challinor, *Phys. Rept.* **429** (2006) 1 [astro-ph/0601594].
  - [3] T. Okamoto and W. Hu, *Phys. Rev. D* **67** (2003) 083002 [astro-ph/0301031].
  - [4] P. A. R. Ade *et al.* [Planck Collaboration], *Astron. Astrophys.* (2014) [arXiv:1303.5077 [astro-ph.CO]].
  - [5] A. Abdo *et al.* [Fermi-LAT Collab.], *Phys. Rev. Lett.* **104** (2010) 101101.
  - [6] M. Ackermann *et al.* [Fermi LAT Collab.], *Phys. Rev. D* **85** (2012) 083007.
  - [7] P. A. R. Ade *et al.* [Planck Collaboration], *Astron. Astrophys.* (2014) [arXiv:1303.5076 [astro-ph.CO]].
  - [8] <http://fermi.gsfc.nasa.gov/ssc/data/access/lat/BackgroundModels.html>
  - [9] P. L. Nolan *et al.*, *Astrophys. J. Suppl.* **199** (2012) 31.
  - [10] E. Hivon *et al.*, *Astrophys. J.* **567** (2002) 2 [astro-ph/0105302].
  - [11] G. Chon *et al.*, *Mon. Not. Roy. Astron. Soc.* **350** (2004) 914 [astro-ph/0303414].
  - [12] I. Szapudi, S. Prunet and S. Colombi, *Astrophys. J.* **561** (2001) L11.
  - [13] G. Efstathiou, *Mon. Not. Roy. Astron. Soc.* **349** (2004) 603 [astro-ph/0307515].
  - [14] M. Ackermann *et al.* [Fermi-LAT Collaboration], *Astrophys. J. Suppl.* **203** (2012) 4 [arXiv:1206.1896 [astro-ph.IM]].
  - [15] D. N. Limber, *Ap.J.* (1953) 117, 134L; N. Kaiser, *Ap.J.* 388 (1992) 272; N. Kaiser, *Ap.J.* 498 (1998) 26.
  - [16] A. Cooray and R. K. Sheth, *Phys. Rept.* **372** (2002) 1.
  - [17] N. Fornengo and M. Regis, *Front. Physics* **2** (2014) 6 [arXiv:1312.4835 [astro-ph.CO]].
  - [18] M. Bartelmann, *Class. Quant. Grav.* **27** (2010) 233001.
  - [19] S. Camera, M. Fornasa, N. Fornengo and M. Regis, *Astrophys. J.* **771** (2013) L5 [arXiv:1212.5018 [astro-ph.CO]].
  - [20] F. Stecker *et al.*, *Astrophys. J.* **658** (2007) 1392.
  - [21] M. Di Mauro *et al.*, *Astrophys. J.* **780** (2014) 161 [arXiv:1304.0908 [astro-ph.HE]].

- [22] M. Ajello *et al.*, *Astrophys. J.* **780** (2014) 73 [arXiv:1310.0006 [astro-ph.CO]].
- [23] M. Ajello *et al.* *Astrophys. J.* **751** (2012) 108.
- [24] C. Gruppioni *et al.*, *Mon. Not. Roy. Astron. Soc.* **432** (2013) 23, [arXiv:1302.5209 [astro-ph.CO]].
- [25] M. Ackermann *et al.* [Fermi LAT Collab.], *Astrophys. J.* **755** (2012) 164.
- [26] R. Sheth and G. Tormen, *MNRAS* **308** (1999) 119.
- [27] S. Camera, M. Fornasa, N. Fornengo and M. Regis, arXiv preprint, 2014, [astro-ph.CO].